Fractional Calculus Guidance Algorithm in a Hypersonic Pursuit-Evasion Game

Jian Chen[#,*], Qilun Zhao[@], Zixuan Liang[@], Peng Li[l], Zhang Ren[@], and Yongjun Zheng[#]

[#]College of Engineering, China Agricultural University, Beijing - 100 083, China
[@]School of Automation Science and Electrical Engineering, Science and Technology on Aircraft Control Laboratory, Beihang University, Beijing - 10 0191, China
[l]Department of Mechanical Engineering, University of Houston, Houston - 77 204, USA
[*]E-mail: chenjian@buaa.edu.cn

ABSTRACT

Aiming at intercepting a hypersonic weapon in a hypersonic pursuit-evasion game, this paper presents a fractional calculus guidance algorithm based on a nonlinear proportional and differential guidance law. First, under the premise of without increasing the complexity degree of the guidance system against a hypersonic manoeuvering target, the principle that the differential signal of the line-of-sight rate is more sensitive to the target manoeuver than the line-of-sight rate is employed as the guidelines to design the guidance law. A nonlinear proportional and differential guidance law (NPDG) is designed by using the differential derivative of the line-of-sight rate from a nonlinear tracking differentiator. By using the differential definition of fractional calculus, on the basis of the NPDG, a fractional calculus guidance law (FCG) is proposed. According to relative motions between the interceptor and target, the guidance system stability condition with the FCG is given and quantitative values are also proposed for the parameters of the FCG. Under different target manoeuver conditions and noisy conditions, the interception accuracy and robustness of these two guidance laws are analysed. Numerical experimental results demonstrate that the proposed guidance algorithms effectively reduce the miss distance against target manoeuvers. Compared with the NPDG, a stronger robustness of the FCG is shown under noisy condition.

Keywords: Pursuit-evasion game; Target manoeuver; Fractional calculus; Guidance law; Hypersonic weapon

1. INTRODUCTION

In recent years, many countries are forcefully developing hypersonic weapons in near space, such as United States (AHW, HTV-2, X-51 and X-43), India (HSTDV and RLV-TD), China (WU-14) and Russia (GLL-31). Because of its ultra-high speed and non-fixed trajectory, the hypersonic weapon has become a great strategic threat to the homeland air defence[1-5]. The hypersonic vehicle flies over 5 Mach in the near space of 20 km to 100 km. Compared with the ballistic missile, the hypersonic weapon is usually designed in a lifting body to obtain stronger manoeuverability. Traditional defense systems against cruise missiles in the atmospheric cannot reach the near space. Thereby, the near space hypersonic weapon is a threat to the current defence system.

There are mainly two kinds of hypersonic vehicles. One is the air-breathing cruise vehicle[6]. Its manoeuverability is relatively weaker, thus its interception is relatively easier as its trajectory is predictable. The other is the gliding entry vehicle[7]. At the entry stage, its velocity is up to 25 Mach at maximum. In the entry phase, it is able to glide thousands of kilometers in the near space without any power. In the terminal phase, a dive attack is performed to the target on the ground[8]. Therefore, its trajectory is not predictable and its interception is a challenge. A

lot of research on entry guidance techniques with no-fly zones constraints have been conducted for hypersonic weapons[9,10]. However, there are few research works on intercepting these vehicles[11]. Consequently, new technical challenges are raised to intercept these weapons and advanced guidance law is needed to provide a high interception accuracy against a hypersonic manoeuverable target[12].

Being applied to intercept the hypersonic weapon, the popular proportional navigation guidance law (PNG) has a major defect that the guidance command lags behind the target manoeuver[13]. Hence, the PNG is less accurate and its performance is unsatisfied with intercepting a manoeuverable target. PID controller is widely used in practice because of its simple formulation and guaranteed performance. Actually, PNG is a proportional controller which belongs to the family of PID controllers. Since the guidance command produced by the PNG lags behind the target manoeuver, and the $\ddot{q}$ reflects the target manoeuver, it is reasonable to add a differential term $K_D \cdot \ddot{q}$ to the PNG. Thus, the proportional and differential (PD) control technique is employed to design the guidance law in a hypersonic pursuit-evasion game.

By introducing the fractional calculus to the PID control, the fractional order PID control has become an emerging field since 1990s[14]. The fractional calculus is a generalisation of the classical an integer-order calculus. There are mainly three Fractional calculus definitions, including Riemann Liouville

(RL) definition, Grümwald Letnikov (GL) definition, and Caputo definition. As the proposition of the gamma function and precise methods for solving fractional order equations appear, the fractional calculus has been applied in controller design field[15,16]. Similar to an integer order PID controller, the formulation of fractional order PID controller can be divided into PI$^\lambda$, PD$^\mu$ and PI$^\lambda$D$^\mu$ (λ and μ represent fractional orders). Compared to an integer order PD controller concerned in this paper, the a fractional order PD$^\mu$ controller has the following advantages. First, a fractional order controller has greater control flexibility. PD$^\mu$ has three parameters, including proportional and differential gains, and a differential order. The choice of a differential fractional order makes it more flexible than an integer order PD controller. Second, a fractional order controller makes the system more robust. The fractional order controller is not sensitive to the parameter perturbation of the controller itself and controlled plant. In other words, as long as the system parameters vary within a certain range, a fractional order controller can perform well.

To sum up, the fractional order PID controller not only inherits all the advantages of the classic integer order PID controller, but also makes a great breakthrough. The memory function and stability characteristic make the fractional order PID controller widely apply in the field of aircraft guidance and control[15,16], such as pitch loop control of a vertical takeoff and landing Unmanned aerial vehicle (UAV)[17], roll control of a small fixed-wing UAV[18], perturbed UAV roll control[19], hypersonic vehicle attitude control[20], aircraft pitch control[21], deployment control of a space tether system[22], position control of a one-DOF flight motion table[23], and vibration attenuation to airplane wings[24]. The viscosity of the atmosphere interacting with air vehicles has endued aircrafts the aerodynamics similar to the fractional order systems, thus the fractional order PID control theory is appropriate to design the aircraft guidance and control system.

Han[17], *et al.* designed a fractional order strategy to control the pitch loop of a vertical takeoff and landing UAV. Simulations verified that the proposed controller was superior to an integer order PI controller based on the modified Ziegler-Nichols tuning rule and a general integer order PID controller in robustness and disturbance rejection. Luo[18], *et al.* developed a fractional order PI$^\lambda$ controller to control the roll channel of a small fixed-wing UAV. From both simulation and real flight experiments, the fractional order controller outperformed the modified Ziegler-Nichols PI and the integer-order PID controllers. Seyedtabaii applied a fractional order PID controller to the roll control of a small UAV in dealing with system uncertainties, where the aerodynamic parameters are often approximated roughly[19]. Song[20], *et al.* proposed a nonlinear fractional order proportion integral derivative (NFOPI$^\lambda$D$^\mu$) active disturbance rejection control strategy for the hypersonic vehicle flight control. The proposed method was composed of a tracking-differentiator, a NFOPI$^\lambda$D$^\mu$ controller and an extended state observer. Simulations showed that the proposed method made the hypersonic vehicle nonlinear model track desired commands fast and accurately, and have robustness against disturbances. Kumar[21], *et al.* developed the fractional order PID (FOPID) and integer order PID controllers

using multi-objective optimisation based on the Bat algorithm and differential evolution technique. The proposed controllers were applied to the aircraft pitch control. Simulations demonstrated that the FOPID using multi-objective bat-algorithm optimisation had better performances than others. Sun & Zhu[22] proposed a fractional order tension control law for deployment control of a space tether system and the stability was proved. Zarei[23], *et al.* realised a fractional order controller for position control of a one-DOF flight motion table. The flight motion table was used for simulating the rotational movement of flying vehicles. Experiments showed using the fractional order controller to tracking of a position profile was feasible and real-time. Birs[24], *et al.* presented a tuning method of a fractional order proportional derivative controller based on three points of the magnitude Bode diagram for vibration attenuation. An aluminum beam replicating an airplane wing verified the proposed controller.

However, there is not much effort dealing with the pursuit-evasion problem against target manoeuver and guidance noise with the fractional order PID controller. Ye[25], *et al.* presented a 3D extended PN guidance law for intercepting a manoeuvering target based on fractional order PID control theory and demonstrated that the air-to-air missile had a smaller miss distance to a manoeuvering target. However, in their research, the velocity of the missile was twice as much as that of the target, and the noise impacting on the guidance state (such as the line-of-sight rate) was not under consideration, which limited the proposed algorithm's practical engineering applications. For this reason, based on a nonlinear proportional and differential guidance law (NPDG) and the fractional calculus technique, a fractional calculus guidance law (FCG) is proposed to intercept a hypersonic manoeuverable target in this paper. It is assumed that the velocity of the interceptor is same as that of the hypersonic target, which means the target can evade as fast as the interceptor, and the guidance noise of the line-of-sight rate is considered.

2. GUIDANCE LAW DESIGN
2.1 Introduction of the NPDG
The PNG is given by

$$a_M(t) = K_P V_R(t)\dot{q}(t) \tag{1}$$

where $a_M(t)$ is the normal acceleration command of the interceptor; $V_R(t)$ is the approaching velocity of the interceptor towards the target; $\dot{q}$ is the line-of-sight (LOS) angular rate; K_P is the proportional coefficient, in the range of 3 to 6 under the consideration of system stability.

In order to restrain the unfavourable effect from the target manoeuver, the LOS angular acceleration $\ddot{q}$ is taken into account, and a nonlinear proportional and differential guidance law (NPDG) is proposed as

$$a_M(t) = K_P V_R(t)\dot{q}(t) + K_D V_R(t)\ddot{q}(t) \tag{2}$$

where K_D is the differential coefficient.

A nonlinear tracking differentiator is used to estimate $\ddot{q}$. The state equation is given by

$$\begin{cases} \dot{x}_1 = x_2, \\ \dot{x}_2 = -K\,\mathrm{sgn}\left(\dfrac{x_1 - \dot{q}_m + |x_2|x_2}{2K}\right), \end{cases} \tag{3}$$

where $\dot{q}_m(t)$ is the LOS rate measured by the seeker; $\dot{q}_m(t)$ and $\ddot{q}_m(t)$ are estimated by x_1 and x_2, namely $x_1 = \hat{\dot{q}}_m(t)$ and $x_2 = \hat{\ddot{q}}_m(t)$; K is the coefficient of the estimator.

The contradiction on selecting the value of K is inevitable: the larger K is, the more precise the estimation is and the less the phase lag is, but the noisier the estimation is. Therefore, a fractional calculus guidance law is proposed.

2.2 Design of the FCG

According to the classic definition of an integer derivative of a continuous function, the definition of Grümwald Letnikov (GL) fractional differential to construct the FCG is given by

$$_a^G D_t^\mu f(t) = \lim_{h \to 0} \frac{1}{h^\mu} \sum_{k=0}^{\frac{t-a}{h}} (-1)^k \frac{\Gamma(\mu+1)}{k!\,\Gamma(\mu-k+1)} f(t-kh) \qquad (4)$$

which makes it extend from an integer-order derivative to a fractional derivative.

If dividing the continuous interval $[a, t]$ of the signal $f(t)$ with the unit $h=1$, and setting $n \in \{1, 2, \ldots, t-a\}$, the difference equation of the fractional differential of $f(t)$ is obtained as

$$\frac{d^\mu f(t)}{dt^\mu} \approx f(t) + (-\mu)f(t-1) +$$
$$\frac{(-\mu)(-\mu+1)}{2} f(t-2) + \ldots + \qquad (5)$$
$$\frac{\Gamma(-\mu+1)}{n!\,\Gamma(-\mu+n+1)} f(t-n).$$

According to definitions of the NPDG and GL, the FCG is proposed as

$$a_M(t) = K_P V_R(t) x(t) + K_D V_R(t) \frac{d^\mu x(t)}{dt^\mu} \qquad (6)$$

where $x(t) = \dot{q}(t)$; $\dfrac{d^\mu x(t)}{dt^\mu}$ is the fractional calculus term of $x(t)$; μ is the fractional order.

According to the GL definition, in the FCG, the fractional differential signal of $\dot{q}$ in the next step relates to the current and previous states. However, in the NPDG, the signal $\ddot{q}$ in the next step only relates to the current state. It indicates that the fractional calculus term is a filter with a characteristic similar to the 'memory'. The FCG works as an effective filter, and is less sensitive to the noises and more resistant to disturbances.

2.3 System Stability Condition

As shown in Fig. 1, assuming that the interceptor and target fly in the same attack plane XOY, M and T denote the interceptor and target; θ_M and θ_T represent flight path angles of the interceptor and target; η_M and η_T represent their heading angles; V_M and V_T represent their velocities; R represents the relative distance between them; q is the line-of-sight angle of the interceptor.

The relative motion equations are given by

$$\dot{q} = \frac{1}{R}(V_M \sin \eta_M - V_T \sin \eta_T) \qquad (7)$$

$$V_R = \dot{R} = -V_M \cos \eta_M + V_T \cos \eta_T \qquad (8)$$

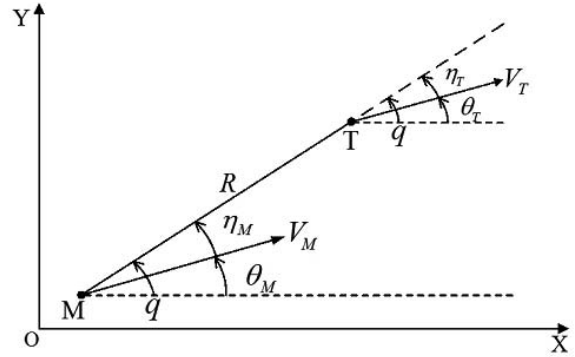$$q = \theta_M + \eta_M = \theta_T + \eta_T \qquad (9)$$

Figure 1. Planar endgame engagement geometry.

Differentiating Eqn. (7), and substituting Eqn. (8) and Eqn. (9) into it, we have

$$R\ddot{q} + 2\dot{R}\dot{q} = \dot{V}_M \sin(\dot{q} - \dot{\theta}_M) - \dot{V}_T \sin(\dot{q} - \dot{\theta}_T)$$
$$+ \dot{\theta}_T V_T \cos(\dot{q} - \dot{\theta}_T) - \dot{\theta}_M V_M \cos(\dot{q} - \dot{\theta}_M). \qquad (10)$$

(1) Linearisation

For a nonlinear problem Eqn. (10), classic stability analysis theories such as the Routh Hurwitz stability criterion for linear systems cannot be applied to it directly. The linearisation must be done at first.

Considering the practical situation, the values of $\dot{V}_M$, $\dot{V}_T$ and $\dot{\theta}_T$ will approach zero in the endgame[26]. Then the nonlinear system Eqn. (10) can be simplified into a linear system:

$$R\ddot{q} + 2\dot{R}\dot{q} \approx -\dot{\theta}_M V_M \cos(q - \theta_M) \qquad (11)$$

From Eqn (11), the transfer function of the guidance system is obtained as

$$\frac{\dot{q}(s)}{\dot{\theta}_M(s)} = \frac{-V_M \cos(q - \theta_M)}{Rs + 2\dot{R}} = \frac{-K_G}{T_G - 1} \qquad (12)$$

where

$$K_G = \frac{V_M \cos(q - \theta_M)}{2|\dot{R}|}, \quad T_G = \frac{R}{2|\dot{R}|}$$

Thus, we get

$$\dot{q}(s) = \frac{-K_G}{T_G s - 1} \dot{\theta}_M(s) \qquad (13)$$

From Eqn (6), since $a_M = V_M \dot{\theta}_M$, we have

$$\dot{\theta}_M = \frac{V_R}{V_M}(K_P \dot{q} + K_D \dot{q} s^\mu) \qquad (14)$$

Substituting Eqn. (14) into Eqn. (13), the characteristic equation of the fractional calculus guidance system comes to

$$\frac{V_R}{V_M} K_G K_D s^\mu + T_G s + \left(\frac{V_R}{V_M} K_G K_P - 1\right) = 0 \qquad (15)$$

(2) Stability analysis

In stability analysis of Eqn. (15), the Hurwitz stability criterion is appropriate to be employed.

Lemma 1 Hurwitz stability criterion[27]

For an nth-degree polynomial characteristic equation:
$$D(s) = a_0 s^n + a_1 s^{n-1} + \cdots + a_{n-1}s + a_n = 0 \quad (a_0 > 0) \qquad (16)$$
The necessary and sufficient stability condition of the

system Eqn. (16) comes to

$$\Delta_1 = a_1 > 0, \quad \Delta_2 = \begin{vmatrix} a_1 & a_3 \\ a_0 & a_2 \end{vmatrix} > 0, \quad \Delta_3 = \begin{vmatrix} a_1 & a_3 & a_5 \\ a_0 & a_2 & a_4 \\ 0 & a_1 & a_3 \end{vmatrix} > 0, \cdots, \Delta_n > 0.$$

(17)

That is, the order principal minor determinants and the main determinant of the system Eqn. (16) are positive.

Thus, based on the Hurwitz stability criterion, the necessary and sufficient stability condition of the system Eqn. (15) comes to

$$a_0 = \frac{V_R}{V_M} K_G K_D > 0$$

(18)

$$\Delta_1 = a_1 = T_G > 0$$

(19)

$$\Delta_2 = \begin{vmatrix} a_1 & a_3 \\ a_0 & a_2 \end{vmatrix} = \begin{vmatrix} T_G & 0 \\ \frac{V_R}{V_M} K_G K_D & \frac{V_R}{V_M} K_G K_P - 1 \end{vmatrix} = T_G \times \left(\frac{V_R}{V_M} K_G K_P - 1 \right) > 0.$$

(20)

That is

$$\begin{cases} \dfrac{V_R}{V_M} K_G K_D > 0, \\ \quad T_G > 0, \\ \dfrac{V_R}{V_M} K_G K_P - 1 > 0. \end{cases}$$

(21)

Since $K_P > 0$ and $K_D > 0$, K_P can be preset as 4. As a consequence, we have $\cos(q-\theta_M) > 0.5$, i.e. $\cos\eta_M > 0.5$. It concludes that:

Theorem 1 when the interceptor's heading angle η_M is in the range of -60° to +60°, the fractional calculus guidance system remains stable.

3. NUMERICAL SIMULATIONS

3.1 Simulations Design

For intercepting a hypersonic weapon, a space-based surveillance satellite and a ground-based X band radar or a marine X band radar should detect the target as early as possible to provide the interceptor enough time to launch from the ground or the aerial carrier. In the terminal phase of a hypersonic weapon, its velocity is too high to be intercepted. For example, a gliding entry vehicle is up to 25 Mach at maximum during a dive attack to the ground target. Thus, the interception is usually designed in the gliding or cruising phase in the near space of a hypersonic weapon before its terminal phase (i.e. before a dive attack happens), then the interceptor-target initial position and heading condition is planned in a head-to-head engagement. In the gliding or cruising phase in the near space of a hypersonic weapon, its velocity is relatively low (about 5 Mach), and its manoeuver amplitude cannot exceed 5 g due to the reduced aerodynamic efficiency since the atmosphere is thin in the near space, but the time instant that the hypersonic weapon starts manoeuvering is flexible and adjustable for evading the interceptor's pursuit. Our preliminary studies and experiments show that it is not good for the hypersonic weapon to start manoeuvering as early as possible during a pursuit-evasion game, and it is better for the

hypersonic weapon to start manoeuvering when the interceptor closes to it in the endgame. For the manoeuvering mode of the hypersonic weapon to evade the interceptor's pursuit, the step manoeuver and square manoeuver are preferred to the ramp manoeuver and sine manoeuver since the formers can provide the hypersonic weapon the maximum evading acceleration instantly.

Based on the analysis above, the simulation parameters for a hypersonic pursuit-evasion game are set as: the interceptor-target initial position and heading condition is planned in a head-to-head engagement, and the initial relative distance R = 30000 m; V_T = 5 Mach, which is along the negative X-axis; V_M = 5 Mach, and its initial direction is aiming at the target, i.e. $\theta_M = q$; the initial LOS angle q is 10°; the interceptor's maximum normal acceleration is 15 g; μ is set as an optimal value of 0.5 by experiences. Obviously, $\eta_M = q - \theta_M = 0° \in [-60°, 60°]$. The fractional calculus guidance system is stable based on Theorem 1.

According to authentic manoeuvering characteristics of a hypersonic weapon in the gliding or cruising phase in the near space when the interceptor closes to it, its manoeuver equations are given by

Case 1: Step manoeuver

$$a_T = 5\mathrm{g}, \quad t \geq 8\sec,$$

(22)

Case 2: Square manoeuver

$$a_T = \begin{cases} 5\mathrm{g}, & t \in [2k+6, 2k+7)\sec, \\ -5\mathrm{g}, & t \in [2k+7, 2k+8)\sec, \end{cases}$$

(23)

where a_T is the norm acceleration of the target, t is the time index and $k \in \mathrm{N}$.

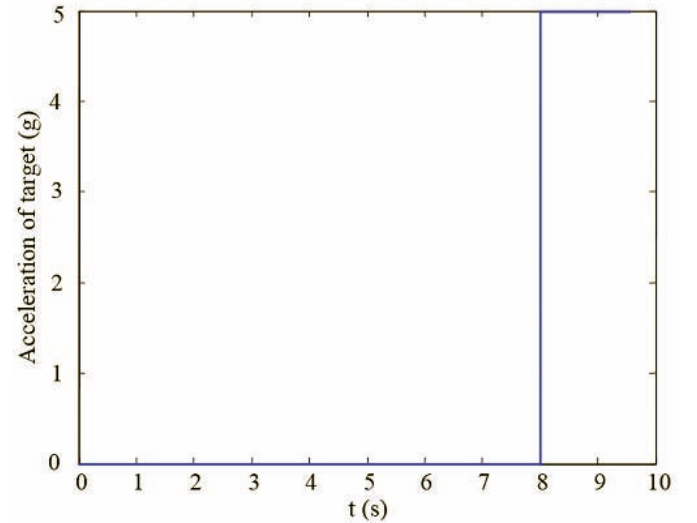The target manoeuvers are shown in Figs. 2 and 3.

Figure 2. Step manoeuver of the target (case 1).

3.2 Interception Accuracy

The trajectories, line-of-sight rates and guidance commands of the interceptor and target are shown in Figs. 4 to 9. From Figs. 4 and 5, since the velocities of the interceptor and target are hypersonic (5 Mach), the amplitude of the target manoeuvers is 5g which cannot change the velocities and trajectories of the target a lot in a limited endgame time. Thus, there is no big difference between the trajectories of the
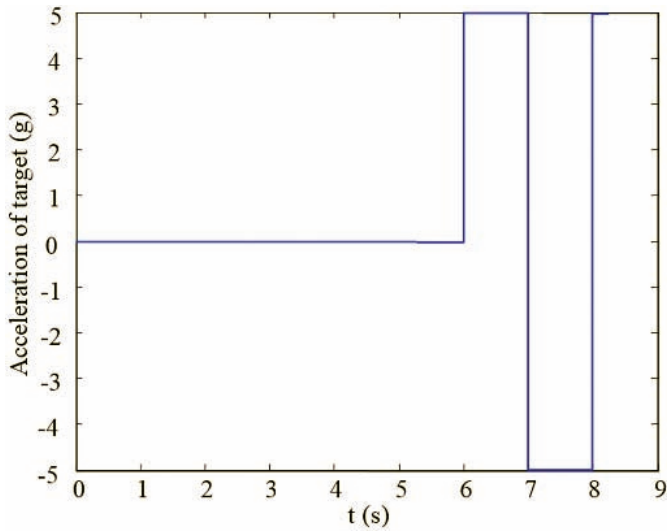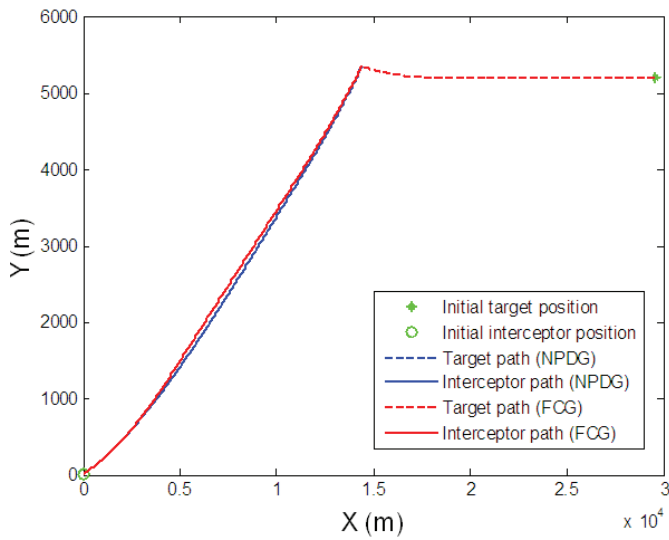
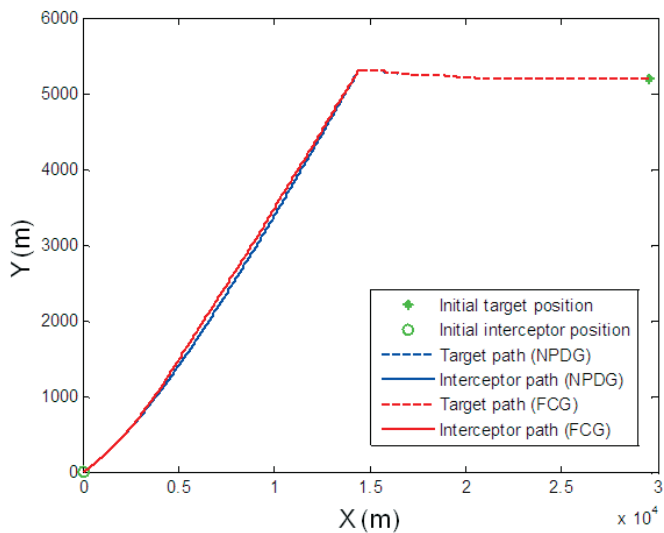**Figure 3. Square manoeuver of the target (case 2).**

target in Figs. 4 and 5. From Figs. 6 and 7, the line-of-sight rates constrained by the FCG are much smaller than those constrained by the NPDG. And the line-of-sight rates of the NPDG are always non-convergent. From Figs. 8 and 9, the guidance commands of the FCG are much smoother than those of the NPDG, which are more appropriate for the interceptor's autopilot to track. The reason is that the NPDG uses a nonlinear tracking differentiator Eqn. (3) to estimate the $\ddot{q}$. In Eqn. (3), K is the coefficient of the estimator. The larger K is, the more precise the estimation is and the less the phase lag is, but the noisier the estimation is. Comparing Fig. 9 with Fig. 8, the guidance commandsof the NPDG in the case 2 are noisier than those of the NPDG in the case 1, which means the target manoeuver of the case 2 is more challenging to the NPDG than that of the case 1. It is also validated by the results in Table 1 that the miss distance of the NPDG in the case 2 is larger than that of the NPDG in the case 1. however, the target manoeuver of the case 2 has little influence on the interception accuracy of the FCG, since the miss distance of the FCG in the case 2 is even smaller than that of the FCG in the case 1.
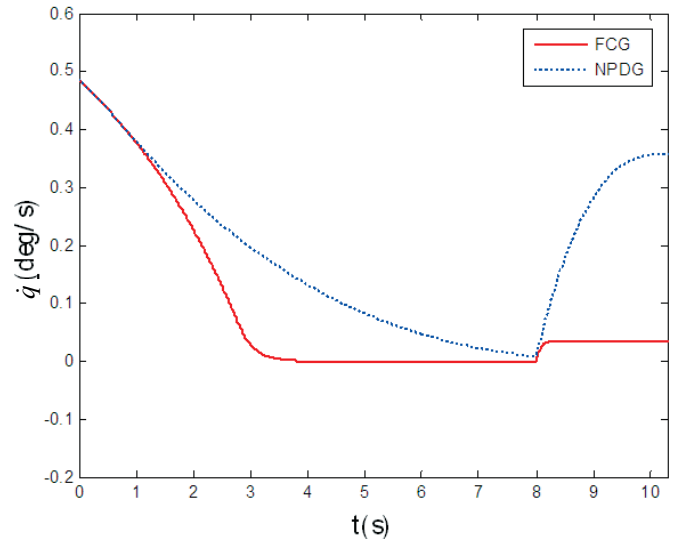

Figure 4. Trajectories of the interceptor and target (case 1).

Figure 6. Line-of-sight rates (case 1).

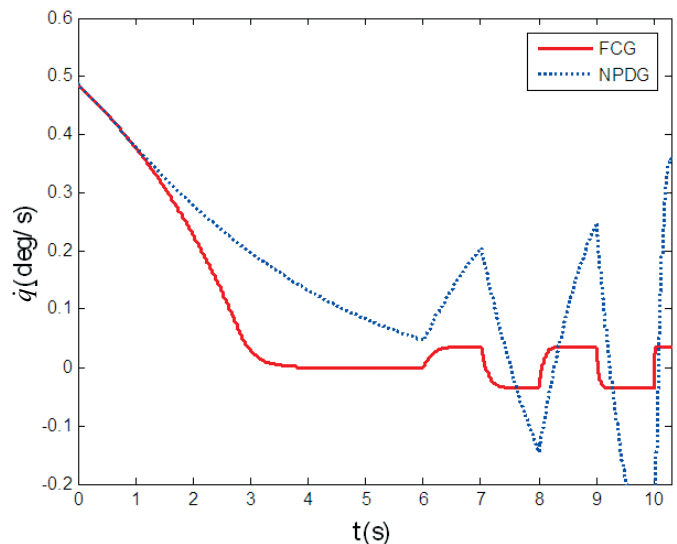**Figure 5. Trajectories of the interceptor and target (case 2).**

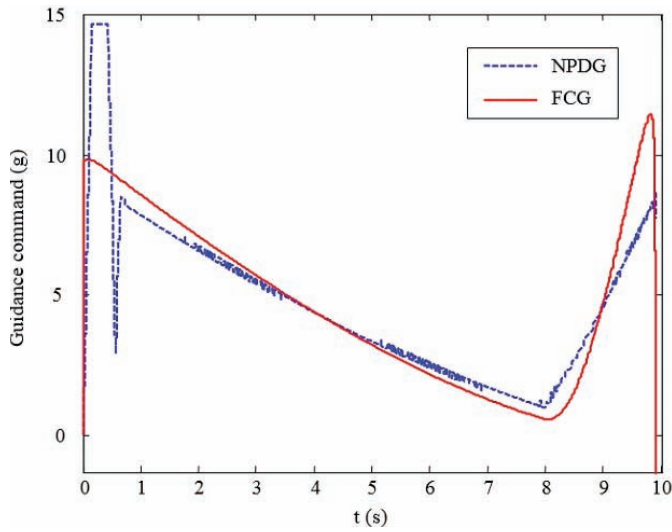**Figure 7. Line-of-sight rates (case 2).**
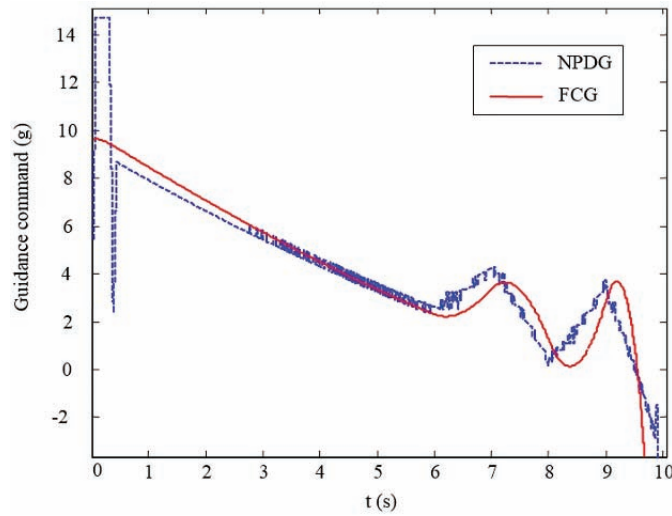
Figure 8. Guidance commands (case 1).

Figure 9. Guidance commands (case 2).

Numerical results are demonstrated in Table 1. The FCG has the minimum miss distance under different scenarios. In the case 1, the miss distance of the FCG is 0.0322 m, which is 91 per cent less than that of the NPDG (0.3406 m). In the case 2, the miss distance of the FCG is 0.0294 m, which is 93 per cent less than that of the NPDG (0.4151 m).

Table 1. Performance evaluation of guidance laws

Guidance law	Case 1: Miss distance (m)	Case 2: Miss distance (m)
NPDG	0.3406	0.4151
FCG	0.0322	0.0294

3.3 Stability

In the case 1, when presetting the simulation parameters, if the initial flight path angle θ_M is set as 40°, 70°, and 75°, respectively, and other parameters remain unchanged, obviously, the heading angle $\eta_M = q - \theta_M$, will be -30°, -60°, and -65°, respectively. The stabilities of the fractional calculus guidance system with the FCG can be analysed based on Theorem 1.

As shown in Figs. 10 to 12, when the heading angle η_M belongs to the closed interval [-60°, 60°], the interceptor can hit and kill the target; when the heading angle η_M is beyond the closed interval [-60°, 60°], the interception mission is failed.

Simulation results are compared and summarised in Table 2. The miss distances increase as the heading angle goes beyond the closed interval [-60°, 60°]; when the heading angle η_M is -60°, it is a critical condition. The experimental results in Table 2 validate the conclusion of Theorem 1.

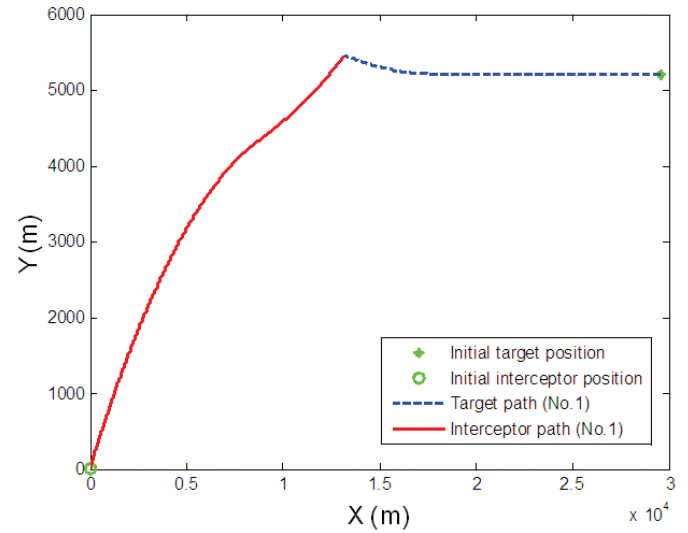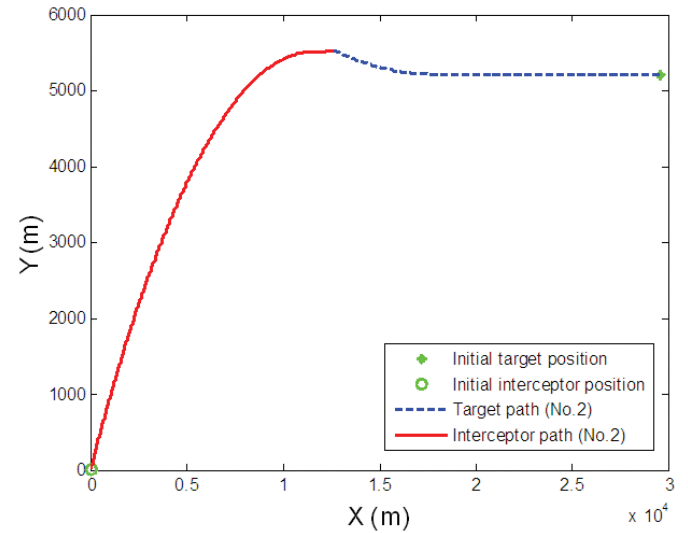**Figure 10. Trajectories of the interceptor and target (No. 1 η_M=-30°).**

Figure 11. Trajectories of the interceptor and target (No. 2 η_M=-60°).

Table 2. Stability analysis

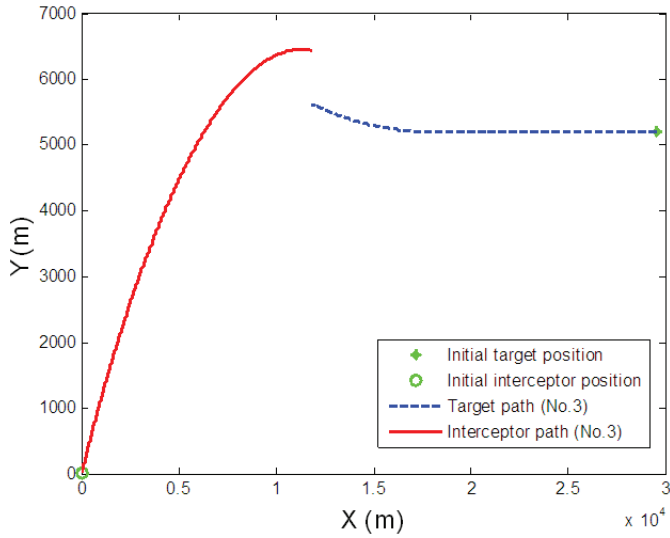| Heading angle η_M(°)	Stability	Miss distance (m)
-30	Stable	0.1060
-60	Stable	8.9125
-65	Unstable	820.7977

Figure 12. Trajectories of the interceptor and target (No. 3 η_M=-65°).

3.4 Robustness

In the case 1, three white noises are added into $\dot{q}$ to run 50 groups of the Monte Carlo simulations, including the amplitudes of 0.5°/s, 1.5°/s and 2.5°/s. The total number of the test times is 50. The miss distances distribution of the NPDG and the FCG with the noise of 0.5°/s, 1.5°/s and 2.5°/s are shown in Figs. 13 to 18.

From Figs. 13, 15, and 17, it can be seen that the miss distances of the NPDG obviously increase as the noise increases. Similarly, from Figs. 14, 16, and 18, the miss distances of the FCG slightly increase as the noise increases. These phenomenon indicate the effect of the noise impacting on the miss distances of both the NPDG and the FCG. Moreover, comparing Fig. 14 with Fig. 13, comparing Fig. 16 with Fig. 15, and comparing Fig. 18 with Fig. 17, the miss distances of the FCG are always smaller than those of the NPDG, which indicates the stronger robustness of the FCG.
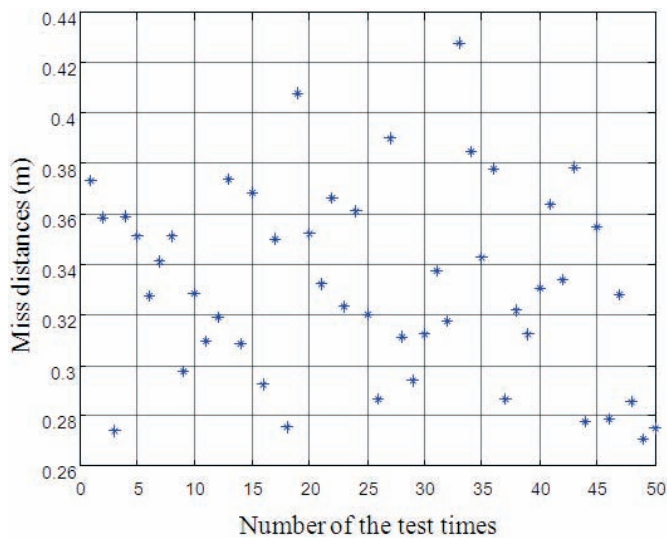

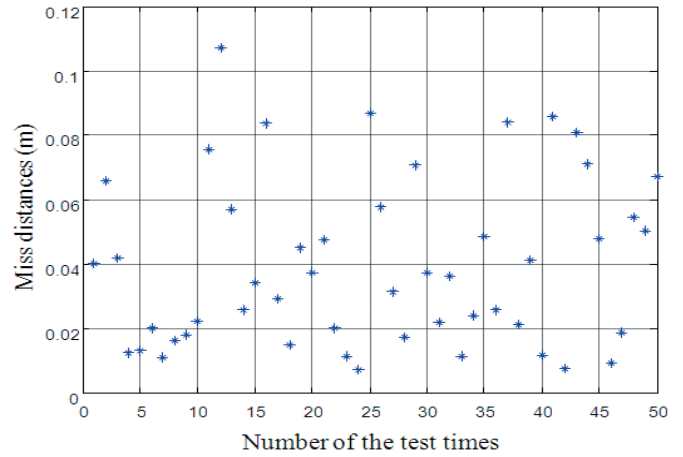Figure 13. Miss distances distribution of the NPDG with the noise of 0.5°/s.

Figure 14. Miss distances distribution of the FCG with the noise of 0.5°/s.
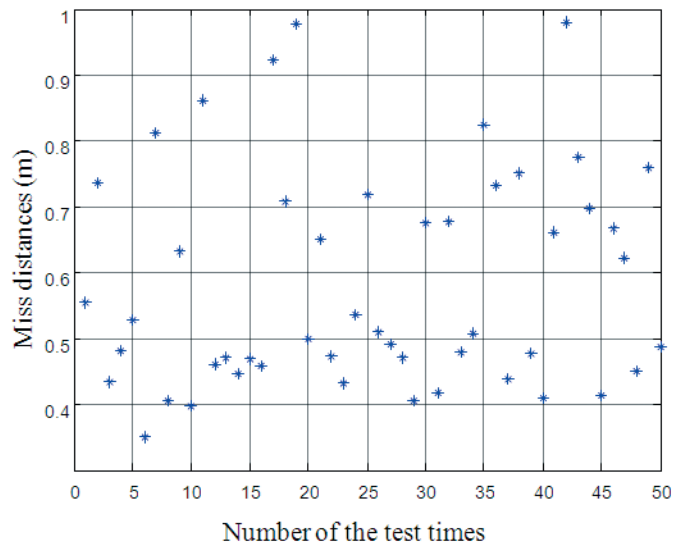

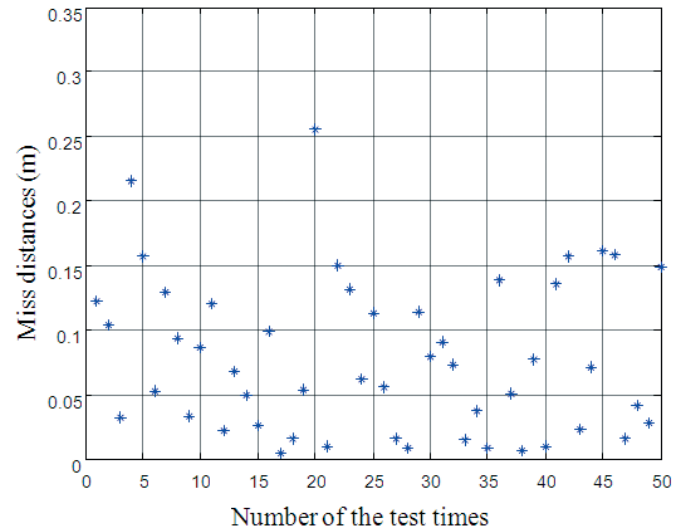Figure 15. Miss distances distribution of the NPDG with the noise of 1.5°/s.

Figure 16. Miss distances distribution of the FCG with the noise of 1.5°/s.

Statistical results are shown in Table 3. The FCG has a less expectation than that of the NPDG: 88 per cent (0.0396 of 0.3322) decrease in the case of 0.5°/s; 87 per cent (0.0786 of 0.5842) decrease in the case of 1.5°/s; and 85 per cent (0.1457 of 1.0092) decrease in the case of 2.5°/s. Obviously, compared with the NPDG, the FCG has a better robustness to the guidance noises.
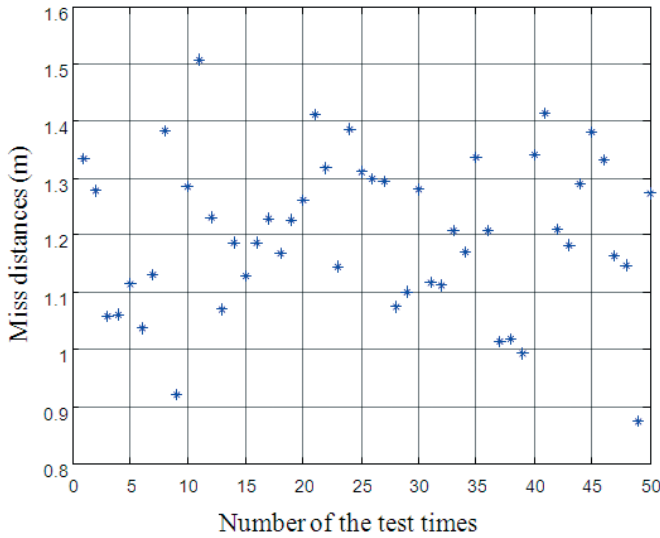

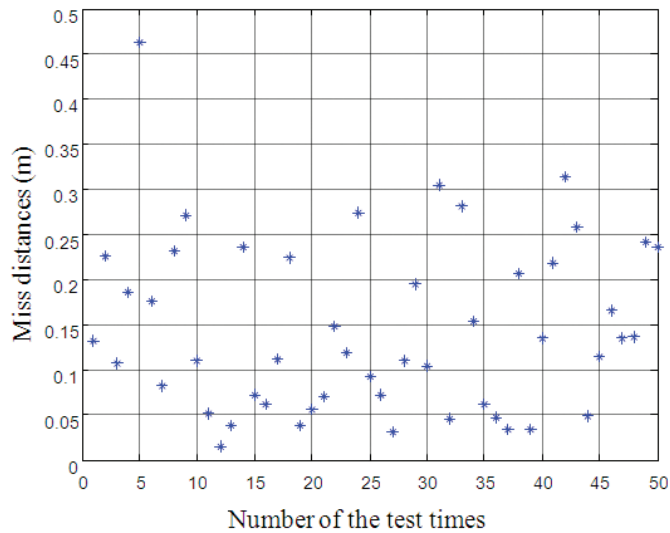**Figure 17.** Miss distances distribution of the NPDG with the noise of 2.5°/s.

Figure 18. Miss distances distribution of the FCG with the noise of 2.5°/s.

Table 3. Statistical results of the miss distances under noisy conditions

Noise (°/s)	Guidance law	Expectation (m)	Variance (m)
0.5	NPDG	0.3322	0.0014
0.5	FCG	0.0396	6.7768e-004
1.5	NPDG	0.5842	0.0274
1.5	FCG	0.0786	0.0036
2.5	NPDG	1.0092	0.2044
2.5	FCG	0.1457	0.0091

To summarise the interception accuracy and robustness experiments, the experimental conclusions can be obtained. The unique filtering properties of the fractional calculus guidance law makes its interception accuracy and robustness perform better. For intercepting a hypersonic weapon, introducing the differential signal of the line-of-sight rate as the guidance information can effectively suppress the target manoeuvers, and has a good robustness, which can become a feasible guidance strategy. The specifications are as follows:

(1) The FCG can improve the guidance accuracy. Compared with the NPDG, it has a better feasibility, since the NPDG requires the measurement of $\ddot{q}$, while this angular acceleration usually cannot be directly measured by the interceptor's seeker. As shown in the guidance commands of the NPDG (Figs. 4 and 5), its tracking differentiator could get into trouble by high-frequency noises. The FCG takes advantage of the numerical method to obtain the fractional differential signal of $\dot{q}$, so as to confront the influence of the target manoeuver.

(2) The FCG has a better robustness than the NPDG. In the FCG, the method obtaining the fractional differential signal of $\dot{q}$ has improved the estimation's precision. The filter properties of the fractional calculus term in the FCG provide the system a good stability in a hypersonic pursuit-evasion game under noisy conditions.

4. CONCLUSIONS

This paper first discusses how to solve the problem of intercepting the hypersonic manoeuvering target without greatly increasing the complexity degree of the guidance system. Based on the axiom that the response to the target manoeuver of the differential signal of the line-of-sight rate is faster than that of the line-of-sight rate, a nonlinear proportional and differential guidance law is designed by using the differential derivative of the line-of-sight rate. Based on the differential definition of the fractional calculus, a fractional calculus guidance law is designed on the basis of the NPDG. In the simulation experiments of the interception accuracy and robustness, both the NPDG and the FCG demonstrate guaranteed guidance performances. The influence of noises impacting on the guidance system is studied. Both of the guidance laws can effectively intercept hypersonic manoeuvering targets while reducing the impact of noise signals. Furthermore, the method obtaining the fractional differential signal of $\dot{q}$ in the FCG is better than the method estimating the $\ddot{q}$ in the NPDG.

In conclusion, under the premise of without greatly increasing the complexity degree of the guidance system, introducing the differential signal of the line-of-sight rate to formulate the novel guidance laws, can meet the precision need to intercept a hypersonic weapon. The FCG is superior to the NPDG in the interception accuracy and the robustness to guidance noises.

REFERENCES

1. Romaniuk, S. N. & Grice, F. The future of US warfare. Taylor & Francis, New York, 2017.
2. Besser, H. L.; Huggins, M.; Zimper, D. & Goge, D. Hypersonic vehicles: State-of-the-art and potential

game changers for future warfare. *In* Brochure of 2016 NATO Science & Technology Symposium, Science & Technology Organization, Brussels, Belgium, 2016.

3. Majumdar, S. BrahMos: A hypersonic future? *Vayu Aerospace Def. Rev.*, 2017, (1), 116.

4. Butt, Y. A hypersonic nuclear war is coming. *New Perspectives Quarterly*, 2016, **33**(1), 51-54.
   doi: 10.1111/npqu.12024

5. Bartles, C. K. Russian threat perception and the ballistic missile defense system. *J. Slavic Military Stud.*, 2017, **30**(2), 152-169.
   doi: 10.1080/13518046.2017.1307016

6. Murugan, T.; De, S. & Thiagarajan, V. Validation of three-dimensional simulation of flow through hypersonic air-breathing engine. *Def. Sci. J.*, 2015, **65**(4), 272-278.
   doi: 10.14429/dsj.65.6979

7. Li, G.; Zhang, H. & Tang, G. Manoeuver characteristics analysis for hypersonic glide vehicles. *Aerospace Sci. Technol.*, 2015, **43**, 321-328.
   doi: 10.1016/j.ast.2015.03.016

8. Xie, D.; Wang, Z. & Zhang, W. A new strategy of guidance command generation for re-entry vehicle. *Def. Sci. J.*, 2013, **63**(1), 93-100.
   doi: 10.14429/dsj.63.2360

9. Wang, T.; Zhang, H. & Tang, G. Predictor-corrector entry guidance with waypoint and no-fly zone constraints. *Acta Astronautica*, 2017, **138**, 10-18.
   doi: 10.1016/j.actaastro.2017.05.009

10. He, R; Liu, L.; Tang, G. & Bao, W. Rapid generation of entry trajectory with multiple no-fly zone constraints. *Advances in Space Research*, 2017, **60**(7), 1430-1442.
    doi: 10.1016/j.asr.2017.06.046

11. Liu, C.; Liu, C. & Tuan, P. Algorithm of impact point prediction for intercepting reentry vehicles. *Def. Sci. J.*, 2016, **56**(2), 129-146.
    doi: 10.14429/dsj.56.1877

12. Vathsal, S. & Sarkar, A. K. Current trends in tactical missile guidance. *Def. Sci. J.*, 2005, **55**(2), 265-280.
    doi: 10.14429/dsj.55.1991

13. Tyan, F. Analysis of general ideal proportional navigation guidance laws. *Asian J. Control*, 2016, **18**(3), 899-919.
    doi: 10.1002/asjc.1205

14. Das, S. Functional fractional calculus. Springer, Berlin, 2011.
    doi: 10.1007/978-3-642-20545-3

15. Chen, Y. Q.; Vinagre, B. M. & Xue, D. Fractional-order systems and controls: fundamentals and applications. Springer, London, 2010.

16. Li, Z; Liu, L; Dehghan, S.; Chen, Y. Q. & Xue, D. A review and evaluation of numerical tools for fractional calculus and fractional order controls. *Int. J. Control*, 2017, **90**(6), 1165-1181.
    doi: 10.1080/00207179.2015.1124290

17. Han, J.; Di, L.; Coopmans, C. & Chen, Y. Q. Pitch loop control of a VTOL UAV using fractional order controller. *J. Intelli. Robotic Sys.*, 2014, **73**(1-4), 187-195.
    doi: 10.1007/s10846-013-9912-9

18. Luo, Y.; Chao, H.; Di, L. & Chen, Y. Q. Lateral directional fractional order (PI)$^\alpha$ control of a small fixed-wing unmanned aerial vehicles: controller designs and flight tests. *IET Control Theory and Applications*, 2011, **5**, 2156-2167.
    doi: 10.1049/iet-cta.2010.0314

19. Seyedtabaii, S. New flat phase margin fractional order PID design: perturbed UAV roll control study. *Robotics Autonomous Sys.*, 2017, **96**, 58-64.
    doi: 10.1016/j.robot.2017.07.003

20. Song, J.; Wang, L.; Cai, G. & Qi, X. Nonlinear fractional order proportion integral derivative active disturbance rejection control method design for hypersonic vehicle attitude control. *Acta Astronautica*, 2015, **111**, 160-169.
    doi: 10.1016/j.actaastro.2015.02.026

21. Kumar, P.; Narayan, S. & Raheja, J. Optimal design of robust fractional order PID for the flight control system. *Int. J. Comput. Appl.*, 2015, **128**(14), 31-35.
    doi: 10.5120/ijca2015906759

22. Sun, G. & Zhu, Z. H. Fractional-order tension control law for deployment of space tether system. *J. Guidance, Control, Dynamics*, 2014, **37**(6), 2057-2061.
    doi: 10.2514/1.G000496

23. Zarei, M.; Arvan, M.; Vali, A. & Behazin, F. Design and implementation of fractional order controller for a one DOF flight motion table. *In* Proceedings of the 36th Chinese Control Conference, IEEE, Dalian, China, 2017.
    doi: 10.23919/ChiCC.2017.8029176

24. Birs, I. R.; Folea, S. & Muresan, C. I. An optimal fractional order controller for vibration attenuation. *In* Proceedings of the 25th Mediterranean Conference on Control and Automation, IEEE, Valletta, Malta, 2017.
    doi: 10.1109/MED.2017.7984221

25. Ye, J.; Lei, H. & Li, J. Novel fractional order calculus extended PN for manoeuvering targets. *Int. J. Aerospace Eng.*, 2017, **2017,** 1-9.
    doi: 10.1155/2017/5931967

26. Ben-Asher, J.Z. & Speyer, J.L. Games in aerospace: homing missile guidance. *Handbook of Dynamic Game Theory*, 2017, 1-28.
    doi: 10.1007/978-3-319-27335-8_25-1

27. Dorf, R. C. & Bishop, R. H. Modern control systems. Pearson, Boston, 2011.

ACKNOWLEDGEMENTS

CONTRIBUTORS

Dr Jian Chen received the BS and PhD in guidance, navigation and control from Beihang University, Beijing, China. He is currently an Associate Professor (PhD Advisor) with the College of Engineering, China Agricultural University, Beijing, China. Before that, he was a research scientist in ASM Technology Limited, Hong Kong, China. And he held the post of research

fellows in University of Houston, USA, and University of Toronto, Canada. His current research interests include guidance, navigation and control of UAVs and robotics.
Contribution in the current study is design, deduction and stability proof of the fractional calculus guidance law for intercepting hypersonic targets.

Mr Qilun Zhao received the BS in automation from Nanjing University of Science and Technology, Nanjing, China. He is currently a PhD candidate with the School of Automation Science and Electrical Engineering, Beihang University, Beijing, China. His current research interests include guidance, navigation and control of hypersonic vehicles.
In the present study he has conducted part of hypersonic-interception simulations.

Dr Zixuan Liang received the BS and PhD in guidance, navigation and control from Beihang University, Beijing, China. He is currently a Postdoctoral Research Fellow with the School of Astronautics, Beihang University. His current research interests include guidance, navigation and control of hypersonic vehicles.
In the present study he has provided characteristics analysis of hypersonic vehicles.

Dr Peng Li received the BS and MS in guidance, navigation and control from Beihang University, Beijing, China. He received the PhD in mechatronics engineering from University of Houston, USA. His current research interests include robust control and embedded control systems.
In the present study he has conducted part of hypersonic-interception simulations.

Dr Zhang Ren received the BS, MS and PhD in aerospace engineering from Northwest Polytechnical University, Xi'an, China. He is currently a Professor with the School of Automation Science and Electrical Engineering, Beihang University, Beijing, China. His current research interests include guidance, navigation and control, fault control systems, and robust control.
In the present study he has provided characteristics analysis of hypersonic vehicles.

Dr Yongjun Zheng received the BS, MS and PhD in mechanical engineering from China Agricultural University, Beijing, China. He is currently an Associate Professor with the College of Engineering, China Agricultural University. His current research interests include fluid analysis of UAVs and intelligent sensing.
In the present study he has conducted part of hypersonic-interception simulations.